Numerical method for inverting 1*s*2*p* resonant inelastic x-ray scattering spectra: Interpretation of hidden electronic excitations in CuO

Günter Dräger[1,*] and Pavel Machek[2]
[1]*Institut für Physik, Martin-Luther-Universität Halle-Wittenberg, Hoher Weg 8, 06120 Halle, Germany*
[2]*Institute of Physics of the ASCR, Cukrovarnická 10, 162 00 Praha 6, Czech Republic*
(Received 30 September 2008; revised manuscript received 3 December 2008; published 13 January 2009)

Direct inversion of resonant inelastic x-ray scattering spectra (RIXSS) has been carried out using a numerical method for solving first-kind Fredholm integral equations. Hereby, the oscillator strength distribution (OSD), which is proportional to the empty density of states at the absorption edge, has been obtained from the experimental Cu 1*s*2*p* RIXSS of CuO. In particular, the inversion of RIXSS measured at incident energies below the *K* level threshold provides OSD having a better resolution than it can be achieved with one of the customary x-ray absorption near-edge structure spectroscopies. This can be explained by the virtual character of the intermediate states at low energy excitation. By means of the presented method a so-called "hidden electronic excitation" of CuO has been identified as a very weak core excitation. Furthermore, numerical interpretation of polarized spectra has revealed the p_y-like character of the excited states in a suitable local reference frame. The obtained results are promising for further applications of the method, preferred in the field of strongly correlated materials.

DOI: 10.1103/PhysRevB.79.033103 PACS number(s): 78.70.Ck, 71.27.+a, 74.72.−h, 78.70.Dm

Core excitations into unoccupied levels are sometimes so weak that they apparently do not leave behind visible features in the x-ray absorption near-edge structure (XANES). However, they can become detectable in the resonant inelastic x-ray scattering spectra (RIXSS) and in this context the term "hidden electronic excitations" is used.[1] The great sensitivity by resonance amplification and the higher energetic resolution as compared with conventional XANES spectroscopies make RIXS spectroscopy a powerful method for investigating unoccupied states in condensed matter, frequently in strongly correlated materials. Among them, divalent CuO with its CuO_4 plaquettes similar to those in the high T_c compounds is a good model system toward the understanding of the electronic structure of these materials.

Recently, some of the studies on CuO have shown the advantages of RIXS compared to other XANES spectroscopies, but they have also left open questions. In Ref. 2 the existence of a pronounced structure in the Cu 1*s*2*p* emission of CuO was discovered for incident energies between 8980 and 8984 eV but without finding a visible counterpart in the corresponding total fluorescence yield (TFY) XANES. Unfortunately, as the experimental data were obtained from a powder sample, the authors were not able to determine the character and symmetry of the "hidden" excited state. Polarized RIXSS on CuO were measured later by Döring *et al.*[3] and they have attributed the above-mentioned RIXS structures to states with 4*p*-like symmetry. In Ref. 4 Hayashi *et al.* derived oscillator strength distributions (OSDs) analytically from the experimental 1*s*2*p* RIXSS and obtained XANES-like spectra in which the lifetime-broadening Γ_{1s} due to the 1*s* core hole was suppressed. They compared the spectra with conventional and high-resolution fluorescent excitation (HRFE) XANES and found that the method revealed weak details in the spectra in the same quality as HRFE. An alternative method to identify even weak spectra structures is based on the interpretation of experimental spectra by means of theoretical ones. In this way Shukla *et al.*[5] were able to identify weak structures in the polarized Cu 1*s*2*p* RIXSS of La_2CuO_4 by comparing them with spectra achieved by means of combined *ab initio* and many-body cluster calculations.

Here we present a numerical method for calculating OSD by inversion of the experimental RIXS emission. The inversion of the Cu 1*s*2*p* RIXSS of polycrystalline and single crystalline CuO provides the OSD in a direct way and enables the identification of hidden excitations as well. Additionally, by comparing to several XANES spectroscopies their efficiency with respect to the present problem has been probed.

In the RIXS process, a transition from the initial state $|i\rangle$ to the final state $|f\rangle$ takes place through intermediate states $|n\rangle$ while the incident photon energy E_1 changes to the emitted or scattered energy E_2. Its intensity $I(E_1,E_2)$ for a 1*s*2*p* RIXS process was deduced by Tulkki and Åberg[6] from the Kramers-Heisenberg equation in a good approximation as follows:

$$I(E_1,E_2) \sim \int \frac{E_2/E_1}{[E_1 - E_L - (E+E_2)]^2 + (\Gamma_L/2)^2} \times \frac{(E_K+E)g_{L,K}\mathrm{OSD}(E)}{(E_K+E-E_1)^2+(\Gamma_K/2)^2} dE. \quad (1)$$

Here, we suppose the oscillator strength $g_{L,K}$ of the $2p \rightarrow 1s$ $K\alpha$ transition to be constant. The oscillator strength distribution OSD(E) is proportional to the empty density of states EDOS(E) and to the probability $p[1s,\mathrm{EDOS}(E)]$ of excitations from 1*s* into empty states at the energy E. The last one will produce no additional structures in the OSD besides the EDOS or, in other words, the OSD reflects the EDOS without essential modification. E_K and E_L are the threshold energies of the 1*s* and 2*p* levels, respectively, and Γ_K and Γ_L their widths at half maximum. E is the kinetic energy of the electron, which is excited from the 1*s* level into

empty discrete or continuous states, described in the whole by the term EDOS(E). According to Eq. (1), the emitted intensity $I(E_2)$ taken at a constant E_1 maps the OSD.

To calculate the OSD from experimental $I(E_2)$ we write Eq. (1) in the form

$$I(E_1,E_2) = \int K(E_2,E)f(E)dE = g(E_2). \tag{2}$$

This is the generic form of a first-kind Fredholm integral equation with the function $f(E)$, which contains the unknown function OSD(E) multiplied by the likewise E-dependent 1s core-level function, here approximated by a Lorentzian. The function $K(E_2,E)$, called the kernel, is a known function of the two variables E_2 and E. In accordance with Eq. (1) it is proportional to the 2p core-level function, which depends solely on the sum $(E+E_2)$ of the two variables. This means that the right-hand side $g(E_2)$ representing the intensity $I(E_2)$ is proportional to the function $f(E)$ mirrored and convoluted with the 2p core-level function, here also approximated by a Lorentzian.

For further numerical treatment of Eq. (1) with the aim of computing the $f(E)$ or OSD(E) function from the experimental $g(E_2)$ or $I(E_2)$ data, respectively, we use a numerical method, which is described in Ref. 7. The method starts with the discretization of the integral equation (2) and with the collocation of the $g(E_2)$ function values with the numbers $g[(E_2)_i]$, i.e., the measured values of $g(E_2)$ at given points $(E_2)_i$,

$$g(E_2) = \int K(E_2,E)f(E)dE$$

$$\simeq \sum_{j=1}^{n} K[(E_2)_i,E_j]f(E_j)\Delta E = g[(E_2)_i], \tag{3}$$

for $i,j=1,\ldots,n$; ΔE is the increment of E. The right-hand side of Eq. (3) represents a system of linear equations, in matrix notation written $\bar{K}\bar{f}=\bar{g}$, where $\bar{K}$ is a $n\times n$ matrix. The elements of $\bar{K}$, $\bar{f}$, and $\bar{g}$ are given by $k_{ij}=K[(E_2)_i,E_j]$, $f_i=f(E_i)$, and $g_i=g[(E_2)_i]$.

If all data were unperturbed and all computations could be done in infinite precision, then the inversion process from g to f would be perfectly possible, providing the solution $\bar{f}=(\bar{K})^{-1}\bar{g}$. In fact, the inversion process is very unstable so that it is impossible to compute $\bar{f}$ by means of a simple inversion. Hence, some kind of stabilization technique is needed in order to change this so-called ill-posed problem into a well-posed one. In the present case the stabilization can be achieved by means of a Tikhonov regularization. Instead of $\bar{K}\bar{f}=\bar{g}$ the equation $(\bar{K}^T\bar{K}+\lambda\bar{I})\bar{f}_\lambda=\bar{K}^T\bar{g}$ has to be solved, giving the approximated solution $\bar{f}_\lambda=(\bar{K}^T\bar{K}+\lambda\bar{I})^{-1}\bar{K}^T\bar{g}$. Here, λ is an always positive regularization parameter, $\bar{I}$ the identity matrix, and $\bar{K}^T$ the transpose of matrix $\bar{K}$. The optimal parameter λ may run over many orders of magnitude depending on the special problem.

We have used the above described method for the study of hidden electronic excitations in CuO. Experimental data have been taken from Ref. 2 with a kind permission by two of the authors (Hayashi and Caliebe). The Cu 1s2p RIXSSs of a CuO powder sample were measured at the X21 hybrid wiggler at NSLS with an overall energy resolution of 1.1 eV. Additional RIXSSs of polycrystalline and single crystalline CuO were measured at the beamlines BW1 and W1 at HASYLAB, DESY. The scattered radiation was monitored using cylindrically[8] and spherically[9] bent Si(440) and Si(444) crystals, respectively, and detected by x-ray sensitive charge coupled devices (CCDs) available in both Johann spectrometers. Some data and results of transmission XANES (TXANES) experiments have been taken from the investigations at the beamlines E4 and A1 at HASYLAB.[10]

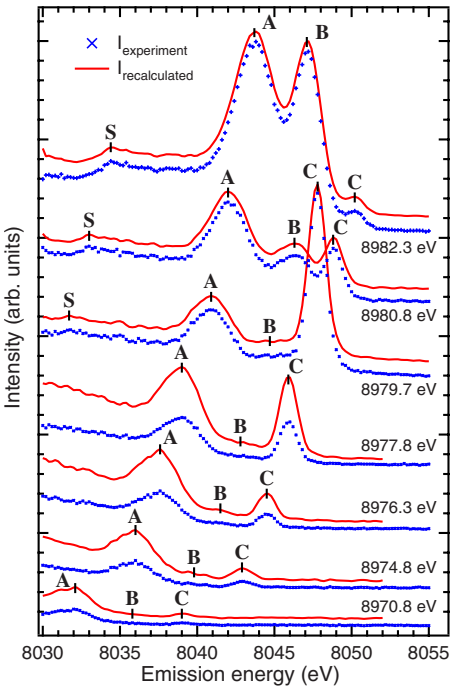

FIG. 1. (Color online) The Cu 1s2$p_{3/2}$ RIXSS of polycrystalline CuO (from Ref. 2) used for the numerical inversion and the RIXSS recalculated from the OSDs in Fig. 2 (details in text).

Figure 1 shows the experimental Cu 1s2$p_{3/2}$ RIXSS of polycrystalline CuO measured at several incident energies E_1 around the Cu K level threshold.[2] The corresponding computed oscillator strength distributions OSD(E_{exc}) are displayed in Fig. 2 in the scale of the excitation energy $E_{exc}=E_K+E$. The inversion of the RIXSS has been carried out using the Tikhonov regularization with a regularization parameter $\lambda=0.015$ and with the quantities $E_K=8979.6$ eV, $E_L=E_{2p_{3/2}}=931.8$ eV, $\Gamma_K=1.55$ eV, and $\Gamma_L=\Gamma_{2p_{3/2}}=0.5$ eV. The obtained results have been used then for the reverse calculation of the RIXSS from the OSD(E_{exc}) by means of the relation $\bar{g}=\bar{K}\bar{f}$. The recalculation provided smoothed curves $I_{recal}(E_2)$, which reproduce the experimental RIXSS $I_{exp}(E_2)$ very well as can be seen in Fig. 1.

The corresponding structures in the RIXSS and in the OSD diagrams can be allocated using the relation $E_{exc}=E_1+E_K-E_L-E_2$. For all fully developed peaks A, B, C, and S in the RIXS spectra the respective positions a, b, c, and s in the OSD diagram have been marked. Vice versa, the position B

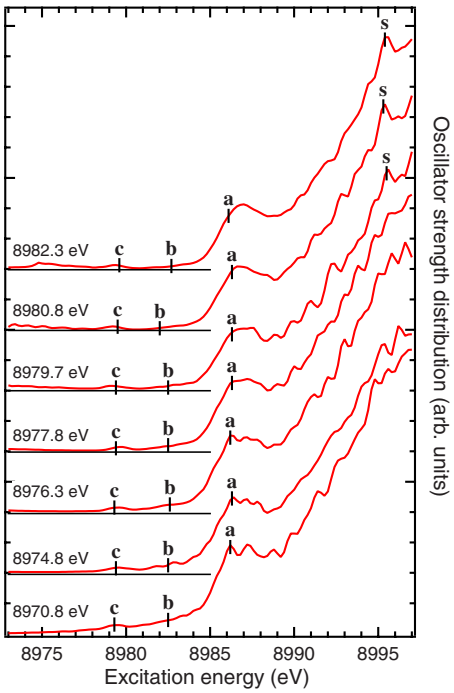

FIG. 2. (Color online) The OSDs obtained by numerical inversion of the experimental RIXSS (Fig. 1).

expected for an averaged b ($\approx$8982.5 eV) has been marked in the RIXSS for incident energies E_1=8979.7, 8977.8, 8974.8, and 8970.8 eV. Peaks A and C in the RIXSS (Fig. 1) fulfill the most important criterions of discrete core excitations: the peaks pass through a resonance and their Raman shift persists also when the resonance has been passed over.[1] These findings can be confirmed and completed by the CuO RIXSS in Refs. 2–4. Peak B, the example of the hidden electronic excitations of CuO, also increases in intensity and shifts to higher emission energy E_2 when the incident energy E_1 increases from 8980.8 to 8982.3 eV. Inspection of the CuO RIXSS in Ref. 4 shows a resonance for this peak at about 8982.5 eV and a pass over of the resonance into the anti-Stokes region. This resonance must come from a very weak core excitation because peak B is still invisible in the RIXSS taken at E_1=8977.8 and 8979.7 eV. Nevertheless, the corresponding b structure is well reproduced (Fig. 2). In the RIXSS with E_1=8976.3, 8974.8, and 8970.8 eV, i.e., spectra with $E_1 < E_K$, at position B some structures are visible again and, therefore, the calculated b structures are better pronounced. This indicates an increase of the resolution at lower E_1, as can be recognized first of all at structure a, which now is very well pronounced. The observation of increasing resolution at lower incident energy can be explained by an increase of the lifetime of the intermediate state $|n\rangle$. Indeed, for $E_1 < E_K$ the state $|n\rangle$ is a virtual one and should have a longer lifetime or a reduced decay probability, respectively, not least because of the lack of the decay channel for fluorescence.

From the Cu K TXANES of CuO and their polarization dependence studied in Ref. 10 we can assign the OSD peak c predominantly to $1s \rightarrow 3d$ electric-quadrupole transitions. All other OSD structures at higher excitation energies should be $1s \rightarrow 4p$ electric-dipole excitations. An assignment of the b

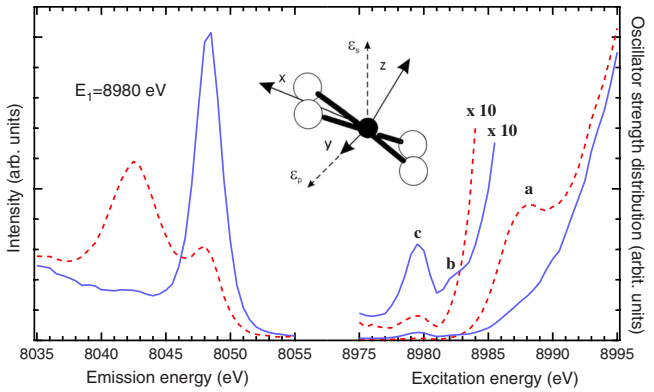

FIG. 3. (Color online) The Cu $1s2p$ RIXSS measured at a CuO single-crystal sample (left side) and the OSD obtained by inversion (right side). The inset shows the orientation of the incident polarizations $\vec{\varepsilon}_p$ and $\vec{\varepsilon}_s$ in the local reference frame xyz with the x axis parallel to the CuO_2 chains. The RIXSS and OSD for $\vec{\varepsilon}_p$ are drawn with solid line; for $\vec{\varepsilon}_s$ with dashed line.

structure with respect to the orbital character of the corresponding electronic states can be carried out by the inversion of polarized RIXSS. For this we have used RIXSS, measured for two different orientations of the incident polarization $\vec{\varepsilon}$ relative to a CuO single-crystal sample.[8] Representatives of the measured RIXSS and calculated OSD(E_{exc}) for both polarizations at incident energy E_1=8980 eV are displayed in Fig. 3. Here the inset shows the orientation of the incident polarizations $\vec{\varepsilon}_p$ and $\vec{\varepsilon}_s$ in a local reference frame xyz defined relative to the central copper atom and the nearest four oxygens of the CuO_4 plaquettes, which form the tilted CuO_2 chains in the CuO crystal structure. According to the dipole selection rules for $1s \rightarrow np$ transitions the incident polarization $\vec{\varepsilon}_p \| y$ maps the p_y-like states of the OSD, whereas the $\vec{\varepsilon}_s$ polarization displays about 60% p_z-like and 40% p_x-like characters in the present case. A comparison of the b structures in Figs. 2 and 3 shows clearly the p_y-like character of the hidden electronic states. On the other hand, the states, which form the structure a, have predominantly $p_{x,z}$ characters. The same is also true for the structures S and s (Figs. 1 and 2). As the immediate oxygen environment around Cu atoms in CuO is similar to that in La_2CuO_4, the RIXSS calculated for La_2CuO_4 in Ref. 5 can be used to interpret the experimental RIXSS of CuO as well. In particular, a qualitative comparison of both spectra identifies the hidden excitation structure B as excitations into $4p_\sigma$ or $4p_{x,y}$ states, respectively. This corresponds essentially to the result obtained by our method.

Comparing finally the different XANES spectroscopies with respect to their ability to resolve the weak and apparently hidden structure b, it can be noticed that by TXANES spectroscopy the structure b cannot be resolved.[10] This statement is true much more for the TFY XANES deduced from our spectra in Ref. 9 and for those in Refs. 2–4 because they are strongly broadened and without any pronounced structures. In the lifetime-broadening-suppressed[4] and HRFE (Refs. 4 and 9) XANESs the b structure is visible but less pronounced as in the inverted RIXSS, measured at $E_1 < E_K$. In general, a decrease of resolution in the HRFE XANES has

been observed with the increase of the incident energy E_1 at which the corresponding HRFE value is measured. This can also be explained by an increase of the lifetime broadening if the intermediate states are excited at higher energies. In contrast, the whole OSD obtained by inversion of RIXSS has a uniform lifetime broadening depending only on the present E_1. Therefore, at $E_1 < E_K$ highly resolved OSD can be obtained.

Summarizing, a powerful numerical method has been used for the inversion of experimental Cu $1s2p$ RIXSS of CuO. The inversion of the spectra, measured at incident energies between 8970 and 8983 eV, reproduces the OSD very well and uncovers the hidden excitation. For incident energies below the K level threshold a clearly better-resolved OSD has been obtained, which can be explained by a reduced lifetime broadening of the virtual intermediate states. The inversion of polarized RIXSS enables the determination of the orbital symmetry of the excitations. For the hidden core excitation at about 8982.5 eV this symmetry is p_y like with respect to the local reference frame of the CuO_4 plaquettes. This means, the corresponding Cu $4p_y$ orbitals lie in the plane of the plaquettes but perpendicular to the axes of the CuO_2 chains. It can be stated that the presented method for inverting experimental RIXSS is promising for further investigations in the field of solid-state and materials physics because it provides OSD having a better resolution than one of the XANES spectroscopies and because it uncovers and identifies even weak structures in the spectra without the need to make *ab initio* calculations. At last, the OSD achieved purely numerically from the experimental spectra can be used to check directly the reliability of *ab initio* calculated density of state (DOS).

This research was supported by Hamburger Synchrotronstrahlungslabor (HASYLAB). The authors are very grateful to Hisashi Hayashi and Wolfgang Caliebe for making available the highly resolved RIXS spectra for numerical interpretation.

*draeger@physik.uni-halle.de

[1] W. Schülke, in *Electron Dynamics by Inelastic X-ray Scattering*, edited by J. Chikawa, J. R. Helliwell, and S. W. Lovesey (Oxford University Press, New York, 2007), Chap. 5.
[2] H. Hayashi, Y. Udagawa, W. A. Caliebe, and C. C. Kao, Phys. Rev. B **66**, 033105 (2002).
[3] G. Döring, C. Sternemann, A. Kaprolat, A. Mattila, K. Hämäläinen, and W. Schülke, Phys. Rev. B **70**, 085115 (2004).
[4] H. Hayashi, R. Takeda, Y. Udagawa, T. Nakamura, H. Miyagawa, H. Shoji, S. Nanao, and N. Kawamura, Phys. Rev. B **68**, 045122 (2003).
[5] A. Shukla, M. Calandra, M. Taguchi, A. Kotani, G. Vanko, and S. W. Cheong, Phys. Rev. Lett. **96**, 077006 (2006).
[6] J. Tulkki and T. Åberg, J. Phys. B **15**, L435 (1982).
[7] P. Ch. Hansen, Numer. Algorithms **29**, 323 (2002).
[8] G. Dräger, Th. Kirchner, S. Bocharov, and C. C. Kao, J. Synchrotron Radiat. **8**, 398 (2001).
[9] E. Welter, P. Machek, G. Dräger, U. Brüggmann, and M. Fröba, J. Synchrotron Radiat. **12**, 448 (2005).
[10] S. Bocharov, T. Kirchner, G. Dräger, O. Šipr, and A. Šimunek, Phys. Rev. B **63**, 045104 (2001).